International Journal of Heat and Mass Transfer 56 (2013) 238–250

Contents lists available at SciVerse ScienceDirect

International Journal of Heat and Mass Transfer

journal homepage: www.elsevier.com/locate/ijhmt

Universal approach to predicting heat transfer coefficient for condensing mini/micro-channel flow

Sung-Min Kim, Issam Mudawar *

Boiling and Two-Phase Flow Laboratory (BTPFL), Purdue University International Electronic Cooling Alliance (PUIECA), Mechanical Engineering Building, 585 Purdue Mall West Lafayette, IN 47907-2088, USA

ARTICLE INFO

Article history:
Received 19 January 2012
Received in revised form 13 September 2012
Accepted 17 September 2012
Available online 27 October 2012

Keywords:
Two-phase flow
Condensation
Mini-channel
Micro-channel

ABSTRACT

A new universal approach to predicting the condensation heat transfer coefficient for mini/micro-channel flows is proposed that is capable of tackling many fluids with drastically different thermophysical properties and very broad ranges of all geometrical and flow parameters of practical interest. This is accomplished by first amassing a consolidated database consisting of 4045 data points from 28 sources. The database consists of single-channel and multi-channel data, 17 different working fluids, hydraulic diameters from 0.424 to 6.22 mm, mass velocities from 53 to 1403 kg/m^2 s, liquid-only Reynolds numbers from 276 to 89,798, qualities from 0 to 1, and reduced pressures from 0.04 to 0.91. An exhaustive assessment of prior correlations shows only two correlations, that are actually intended for macro-channels, provide relatively fair predictions, while mini/micro-channel correlations generally show poor predictions. Two new correlations are proposed, one for predominantly annular flows, and the second for slug and bubbly flows. This approach shows very good predictions of the entire consolidated database, with an overall MAE of 16.0%. It is shown this accuracy is fairly even for different working fluids, and over broad ranges of hydraulic diameter, mass velocity, quality and pressure, and for both single and multiple mini/micro-channels.

1. Introduction

The quest for more compact designs in many modern electronic, defense and aerospace applications has lead to unprecedented increases in the amount of heat dissipation per unit volume. Examples of these applications include high performance computers, electrical vehicle power electronics, avionics, and directed energy laser and microwave weapon systems [1,2]. Both single-phase and two-phase cooling solution have been sought, but the single-phase options are dwindling as heat dissipation densities are exceeding the capabilities of the most promising single-phase cooling solutions.

This limitation explains the recent shift to two-phase cooling solutions. By capitalizing upon a liquid coolant's latent heat rather than sensible heat alone, two-phase cooling schemes can deliver orders of magnitude enhancement in heat transfer coefficient compared to their single-phase counterparts. This explains the recent increase in the number of studies addressing two-phase solutions using a variety of cooling schemes, such as spray [3–5], jet [6–9], and micro-channel [2,10–13], as well as means to enhance surface micro-structure [14]. Nonetheless, two-phase solutions do suffer some shortcomings, including the potential for high pressure drop, susceptibility to flow instabilities, and high cost.

Condensers utilizing mini/micro-channels are an important part of the arsenal of two-phase cooling solutions for applications requiring removal of large, concentrated heat loads. Most condensers are designed to operate in the annular flow regime consisting of a thin liquid film that travels along the walls of a flow channel, driven by shear forces exerted by a central vapor core. Using a small channel diameter serves to increase vapor velocity for a given flow rate, which increases the vapor shear stress, resulting in a thinner liquid film. With sufficient conversion of vapor to liquid along the channel, the increase in liquid film thickness eventually leads to a collapse of the annular regime. In a recent study involving condensation of FC-72 along square micro-channels [15], five distinct flow regimes were identified: smooth-annular, wavy-annular, transition, slug, and bubbly. These regimes are depicted in Fig. 1 in a plot of mass flux versus flow quality. The smooth-annular regime consists of a very thin and fairly smooth annular film that is shear driven by the central vapor core. In the wavy-annular regime, the liquid film is thicker and marred by appreciable interfacial waviness. The transition to slug flow is characterized by intermittent bridging of liquid ligaments from the annular film across the vapor core.

* Corresponding author. Tel.: +1 (765) 494 5705; fax: +1 (765) 494 0539.
E-mail address: mudawar@ecn.purdue.edu (I. Mudawar).
URL: https://engineering.purdue.edu/BTPFL (I. Mudawar).

0017-9310/$ - see front matter © 2012 Elsevier Ltd. All rights reserved.
http://dx.doi.org/10.1016/j.ijheatmasstransfer.2012.09.032

Nomenclature

Bo	Bond number
C	coefficient in Lockhart–Martinelli parameter
C_1, C_2	empirical coefficients
c_p	specific heat at constant pressure
D	tube diameter
D_h	hydraulic diameter
Fr	Froude number
Fr^*	modified Froude number
f	Fanning friction factor
G	mass velocity
g	gravitational acceleration
Ga	Galileo number
h	heat transfer coefficient
h_{fg}	latent heat of vaporization
Ja	Jakob number
J_g^*	dimensionless superficial vapor velocity
Ka	Kapitza number
MAE	mean absolute error
N	number of data points
N_1–N_5	empirical exponents
Nu	Nusselt number
P	pressure
P_{crit}	critical pressure
P_R	reduced pressure, $P_R = P/P_{crit}$
Pr	Prandtl number
Pr_T	turbulent Prandtl number
q''	heat flux
q''_w	heat flux based on micro-channel's cooled perimeter
Re	Reynolds number
Su	Suratman number
T_δ^+	dimensionless boundary layer temperature
u^*	friction velocity
v	specific volume
We	Weber number
We^*	modified Weber number
X	Lockhart–Martinelli parameter
x	thermodynamic equilibrium quality
Δx	quality change
y^+	dimensionless distance normal to the wall, $yu^*/_f$
z	stream-wise coordinate

Greek Symbols

β	channel aspect ratio ($\beta < 1$)
δ	thickness of condensing film
δ^+	dimensionless thickness of condensing film, $\delta u^*/_f$
ε_m	eddy momentum diffusivity
θ	percentage predicted within ±30%
μ	dynamic viscosity
ν	kinematic viscosity
ξ	percentage predicted within ±50%
ρ	density
σ	surface tension
τ_w	wall shear stress
ϕ	two-phase multiplier

Subscripts

3	based on three-sided heat transfer in rectangular channel
4	based on four-sided heat transfer in rectangular channel
ann	annular flow
cir	based on uniform circumferential cooling
exp	experimental (measured)
f	saturated liquid
fo	liquid only
g	saturated vapor
go	vapor only
non-ann	slug and bubbly flow
pred	predicted
sat	saturation
tp	two-phase
tt	turbulent liquid–turbulent vapor
tv	turbulent liquid–laminar vapor
vt	laminar liquid–turbulent vapor
vv	laminar liquid–laminar vapor
w	wall

Achieving very high condensation heat transfer coefficients is by no means the sole concern in arriving at an acceptable cooling scheme. Unfortunately, decreasing channel diameter in pursuit of a higher heat transfer coefficient also increases the condenser's pressure drop, which may compromise overall thermal efficiency. Therefore, the design of a high performance mini/micro-channel condenser demands predictive tools for both pressure drop and condensation heat transfer coefficient. The present study concerns prediction of the condensation heat transfer coefficient.

Studies on two-phase condensing flow in mini/micro-channels [16–43] have resulted in different approaches to predicting the condensation heat transfer coefficient. The vast majority of these studies involve the use or development of semi-empirical correlations [39,41,44–53]. However, these methods have been validated only for specific flow configurations and relatively narrow ranges of operating conditions. Of the different condensation regimes, annular flow has received the most attention. Because annular flow consists of predominantly two separated phases (vapor core and annular liquid film), it lends itself better to theoretical modeling than dispersed flow regimes such as slug and bubbly flows. One method that has shown great promise in modeling annular flow is the control volume approach, where conservation relations are applied separately to the liquid and vapor phases. This approach proved effective in modeling other two-phase flow configurations,

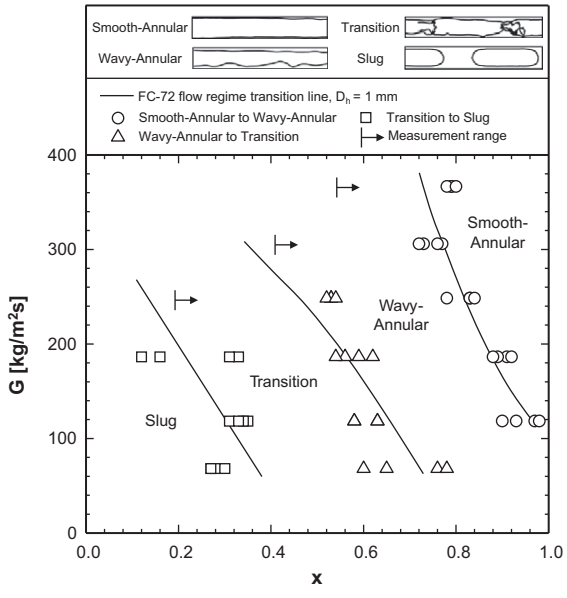

Fig. 1. Two-phase flow regime boundaries for condensation of FC-72 in square micro-channels with D_h = 1 mm [15].

including pool boiling [54,55], and vertical separated flow boiling along short walls [56,57] and long heated walls [58–61]. Recently, the authors of the present study used the control volume approach to construct a new model for annular condensation in mini/micro-channel flows [62]. Unlike this latter study, the primary goal of the present study is to develop a generalized predictive tool for condensation heat transfer coefficient for mini/micro-channel flows applicable to other condensation regimes as well, including wavy laminar, transition to slug, slug, and bubbly.

No study has been published that addresses the development of a generalized correlation for condensation heat transfer coefficient in mini/micro-channels covering a wide range of working fluids with drastically different thermophysical properties, and broad ranges of mass velocity, pressure (atmospheric to near-critical pressures), and channel diameter (tens of micrometers to a few millimeters). As discussed in Ref. [2], development of this predictive tool is the primary motivation for a new initiative at the Purdue University Boiling and Two-Phase Flow Laboratory (PU-BTPFL), including the present study, to (1) consolidate world databases for condensation and flow boiling in mini/micro-channels, and (2) develop universal predictive approaches for both pressure drop and heat transfer coefficient. The approach used here is modeled along the methodology adopted in a previous series of studies at PU-BTPFL concerning the prediction of flow boiling critical heat flux (CHF) [63–66].

In the present study, published condensation heat transfer databases for mini/micro-channel flows are amassed from 28 sources [16–43]. The data are compared to predictions of previous semi-empirical correlations for both macro-channels and mini/micro-channels. A new generalized correlation technique is proposed, which is shown to predict data for very broad ranges of operating conditions and various working fluids with high accuracy.

2. New consolidated mini/micro-channel database

In the present study, a new consolidated database consisting of a total of 4045 condensation heat transfer data points for mini/micro-channels is amassed from 28 sources [16–43]. The database includes 1964 single-channel data points from 17 sources, and 2081 multi-channel data points from 13 sources.

Table 1 provides key information on the individual databases incorporated in the consolidated database in chronological order, along with the number of data points actually adopted. Some of the data are purposely excluded because they do not contribute to the development of a generalized predictive method. For example, only pure liquid data form the databases of Dobson et al. [16,17], Marak [33], and Huang et al. [39] are included in Table 1; any binary mixture, or oil mixture data are excluded. Also excluded are all enhanced tube (e.g., micro-fin tube) data from the databases of Zhang [20], Kim et al. [24], Jang and Hrnjak [26], and Kim et al. [32], as well as barrel, triangular, W-shaped, and N-shaped channels from Agarwal et al. [36], and triangular and semi-circular channels from Derby et al. [42].

Table 1
Condensation heat transfer database for mini/micro-channel flows included in the consolidated database.

Author(s)	Channel geometry*	Channel material	D_h (mm)	Fluid(s)	G (kg/m^{2}s)	Test mode	Data points
Dobson et al. (1993a)	C single, H	Copper	4.57	R134a, R12	75–653	Clocal h Δx = 0.1–0.2	76
Dobson et al. (1993b)	C single, H	Copper	4.57	R22	75–509	Quasi-local h Δx = 0.24 (avg)	32
Dobson (1994)	C single, H	Copper	3.14	R134a, R22	53–807	Quasi-local h Δx = 0.23 (avg)	165
Hirofumi and Webb (1995)	C/R multi, H	Aluminum	0.96–2.13	R134a	200–1403	Quasi-local h Δx = 0.12 (avg)	62
Zhang (1998)	C single/multi, H	Copper, aluminum	2.13, 3.25, 6.20	R134a, R22, R404A	200–1000	Quasi-local h Δx < 0.25	80
Wang (1999)	R multi, H	Aluminum	1.46	R134a	79–761	Local h	748
Yan and Lin (1999)	C multi, H	copper	2.0	R134a	100–200	Quasi-local h small Δx	78
Baird et al. (2003)	C single, H	Copper	1.95	R123	170–570	Local h	143
Kim et al. (2003)	R multi, H	Aluminum	1.41	R410A, R22	200–600	Quasi-local h q'' = 0.5–1.5 W/cm^2	19
Jang and Hrnjak (2004)	C single, H	Copper	6.10	CO_2	197–406	Quasi-local h small Δx	85
Cavallini et al. (2005)	R multi, H	Aluminum	1.4	R410A, R134a	200–1400	Quasi-local h Δx = 0.2–0.3	59
Mitra (2005)	C single, H	Copper	6.22	R410A	200–800	Quasi-local h Δx = 0.21 (avg)	144
Shin and Kim (2005)	C/R single, H	Copper	0.493–1.067	R134a	100–600	Quasi-local h small Δx	237
Andresen (2006)	C single/multi, H	Aluminum, copper	0.76, 1.52, 3.05	R410A	200–800	Quasi-local h Δx = 0.32 (avg)	315
Bandhauer et al. (2006)	C multi, H	Aluminum	0.506, 0.761, 1.524	R134a	150–750	Quasi-local h small Δx	128
Agra and Teke (2008)	C single, H	Copper	4.0	R600a	57–118	Quasi-local h small Δx	50
Kim et al. (2009)	C single, H	Copper	3.48	CO_2	200–800	Quasi-local h small Δx	48
Marak (2009)	C single, VU	Stainless steel	1.0	Methane	162–701	Quasi-local h Δx = 0.04 (avg)	129
Matkovic et al. (2009)	C single, H	Copper	0.96	R134a, R32	100–1200	Local h	161
Park and Hrnjak (2009)	C multi, H	Aluminum	0.89	CO2	200–800	Quasi-local h Δx < 0.3	113
Agarwal et al. (2010)	R multi, H	Aluminum	0.424, 0.762	R134a	150–750	Quasi-local h small Δx	43
Bortolin (2010)	C/R single, H	Copper	0.96, 1.23	R245fa, R134a	67–789	Local h	309
Del Col et al. (2010)	C single, H	Copper	0.96	R1234yf	200–1000	Local h	66
Huang et al. (2010)	C single, H	Copper	1.6, 4.18	R410A	200–600	Quasi-local h Δx = 0.2	35
Oh and Son (2011)	C single, H	Copper	1.77	R22, R134a, R410A	450–1050	Local h	108
Park et al. (2011)	R multi, VD	Aluminum	1.45	R134a, R236fa, R1234ze(E)	100–260	Local h	204
Derby et al. (2012)	R multi, H	Copper	1.0	R134a	75–450	Quasi-local h Δx < 0.3	140
Kim and Mudawar (2012)	R multi, H	Copper	1.0	FC-72	118–367	Local h	268
Total							4045

* C: circular; R: rectangular; H: horizontal; VU: vertical upward; VD: vertical downward.

The generalized correlation sought in this study concerns smooth surfaces, therefore, most of the data in the consolidated database are for smooth surfaces with a relative roughness of 0.001–0.0001. For turbulent flow in particular, only data with a relative roughness of 0.001–0.0001 are included in the consolidated database, therefore, 50 of 179 data points from Marak [33] having relative roughness values in excess of 0.0024 are excluded. Also excluded are hydrophobic (nonwetting) surfaces (e.g., air–water flow on Teflon or Polytetrafluoroethylene (PTFE) surfaces) with a static contact angle larger than 90°.

Also excluded from the consolidated database are any duplicate data in the original databases. Data points were also excluded because of their strong departure from the majority of comparable data, including the condensation data of Bohdal et al. [53] and Agarwall [67]. It should be noted that the database is closely inspected by relying on published data from original sources.

The condensation data included in Table 1 consist of local or quasi-local heat transfer coefficient data. The data of Wang [21], Baird et al. [23], Matkovic et al. [34], Bortolin [37], Del Col et al. [38], Oh and Son [40], Park et al. [41], and Kim and Mudawar [43] correspond to local heat transfer values. The other condensation data in Table 1 correspond to quasi-local heat transfer coefficient averaged over the flow channel. These latter data were measured mostly in short channels or channels associated with lower heat fluxes and therefore small quality decrements along the channel. The average quality value between inlet and outlet of the channel is used to determine the quasi-local heat transfer coefficient value based on the assumption of linear quality variation along the channel. For the quasi-local heat transfer data, the quality change between inlet and outlet of the channel is provided in Table 1, and these values are less than 30% for most individual databases.

Unlike prior databases that have been used to correlate the condensation heat transfer coefficient in mini/micro-channels, the present consolidated database includes a broad range of reduced pressures, from 0.04 to 0.91. Included here are databases covering high reduced pressure values above 0.4 by Dobson et al. [16] (P_R = 0.20–0.41), Hirofumi and Webb [19] (P_R = 0.24–0.47), Zhang [20] (P_R = 0.21–0.49), Wang [21] (P_R = 0.42–0.48), Kim et al. [24] (P_R = 0.35–0.56), Cavallini et al. [25] (P_R = 0.25–0.49), Matkovic et al. [34] (P_R = 0.25–0.43), Huang et al. [39] (P_R = 0.49), Oh and Son [40] (P_R = 0.25–0.49), and Park et al. [41] (P_R = 0.14–0.44). The consolidated database also includes data approaching critical pressure by Mitra [27] (P_R = 0.80–0.90), Andresen [29] (P_R = 0.80–0.90), and Marak [33] (P_R = 0.14–0.91).

In all, the new consolidated database includes 4045 condensation heat transfer coefficient data points with the following coverage:

Working fluid: R12, R123, R1234yf, R1234ze(E), R134a, R22, R236fa, R245fa, R32, R404A, R410A, R600a, FC72, methane, and CO_2
Hydraulic diameter: $0.424 < D_h < 6.22$ mm
Mass velocity: $53 < G < 1403$ kg/m^{2}s
Liquid-only Reynolds number: $276 < \mathrm{Re}_{fo} = GD_h/\mu_f < 89{,}798$
Superficial liquid Reynolds number:
$0 < \mathrm{Re}_f = G(1-x)D_h/\mu_f < 79{,}202$
Superficial vapor Reynolds number: $0 < \mathrm{Re}_g = GxD_h/\mu_g < 247{,}740$
Flow quality: $0 < x < 1$
Reduced pressure: $0.04 < P_R < 0.91$

3. Evaluation of previous correlations

As discussed in [43], experimental mini-/micro-channel condensation data corresponding to annular flow (smooth-annular, wavy-annular, and transition to slug) satisfy the relation $We^* > 7X_{tt}^{0.2}$, which will be discussed later in this paper. As indicated earlier, transition to slug flow is characterized by intermittent bridging of liquid ligaments from the annular film across the vapor core. Figs. 2 and 3 compare 3332 of the 4045 data points of the consolidated database corresponding to annular flow with predictions of previous empirical correlations for both macro-channels [44–49] and mini/micro-channels [39,41,50,51,53], respectively. Thermophysical properties for liquid and vapor used in these figures and all subsequent calculations are based on REFPROP 8.0 software from NIST [68].

The accuracy of individual correlations is evaluated by θ and ξ, the percentages of data points predicted within ±30% and ±50%, respectively, and mean absolute error, defined as

$$MAE = \frac{1}{N}\sum \frac{|h_{tp,pred} - h_{tp,exp}|}{h_{tp,exp}} \times 100\%. \quad (1)$$

Table 2 provides a summary of select condensation heat transfer correlations for annular flow. These correlations can be classified into the following categories: two-phase multiplier-based correlations [44,46,48], and boundary layer-based correlations [39,41,45,47,49–51]. Notice that the correlations of Koyama et al., Huang et al., and Park et al. are based on Haraguchi et al. formulation. The correlations of Wang et al., Koyama et al., and Park et al. are based on data for multi-port mini/micro-channel test sections.

Since the correlations in Table 2 are intended for uniform circumferential cooling in circular tubes or rectangular channels with four-sided cooling, a multiplier is adopted when applying these correlations to condensation data in rectangular channels with three-sided wall cooling, such as Derby et al. [42] and Kim and Mudawar [43], Table 1. Following a technique adopted in Refs. [43,69,70] to correct for three-sided heat transfer, the condensation heat transfer coefficient for three-sided cooling is related to that obtained from that for uniform circumferential cooling by the relation

$$h_{tp} = \left(\frac{Nu_3}{Nu_4}\right) h_{tp,cir}, \quad (2)$$

where $h_{tp,cir}$ is the local heat transfer coefficient based on uniform circumferential cooling obtained from Table 2, and Nu_3 and Nu_4 are Nusselt numbers for thermally developed laminar flow with three-sided and four-sided heat transfer [71], respectively,

$$Nu_3 = 8.235(1 - 1.833\beta + 3.767\beta^2 - 5.814\beta^3 + 5.361\beta^4 - 2.0\beta^5) \quad (3a)$$

and

$$Nu_4 = 8.235(1 - 2.042\beta + 3.085\beta^2 - 2.477\beta^3 + 1.058\beta^4 - 0.186\beta^5). \quad (3b)$$

Fig. 2 shows the macro-channel correlations of Cavallini and Zecchin [45] and Haraguchi et al. [47] highly overpredict the consolidated database. The correlations of Shah [46] and Dobson and Chato [48] overpredict a large fraction of the database, especially for high reduced pressures. Among the macro-channel correlations, those of Akers and Rosson [44] and Moser et al. [49] show relatively good predictions, with MAEs of 27.3%, and 27.7%, respectively. However, Akers and Rosson's correlation underpredicts the data in general, while Moser et al. overpredicts the data corresponding to high reduced pressures.

Fig. 3 shows the consolidated mini/micro-channel database highly underpredicted by Koyama et al. [51] and Park et al. [41], and highly overpredicted by Huang et al. [39] and Bohdal et al. [53]. The correlation of Wang et al. [50] provides relatively good predictions compared to the other mini/micro-channel correlations, although it shows some scatter.

Figs. 2 and 3 highlight an observation made in a previous study by the authors [43]: previous correlations intended for macro-channels generally show better predictions of annular flow

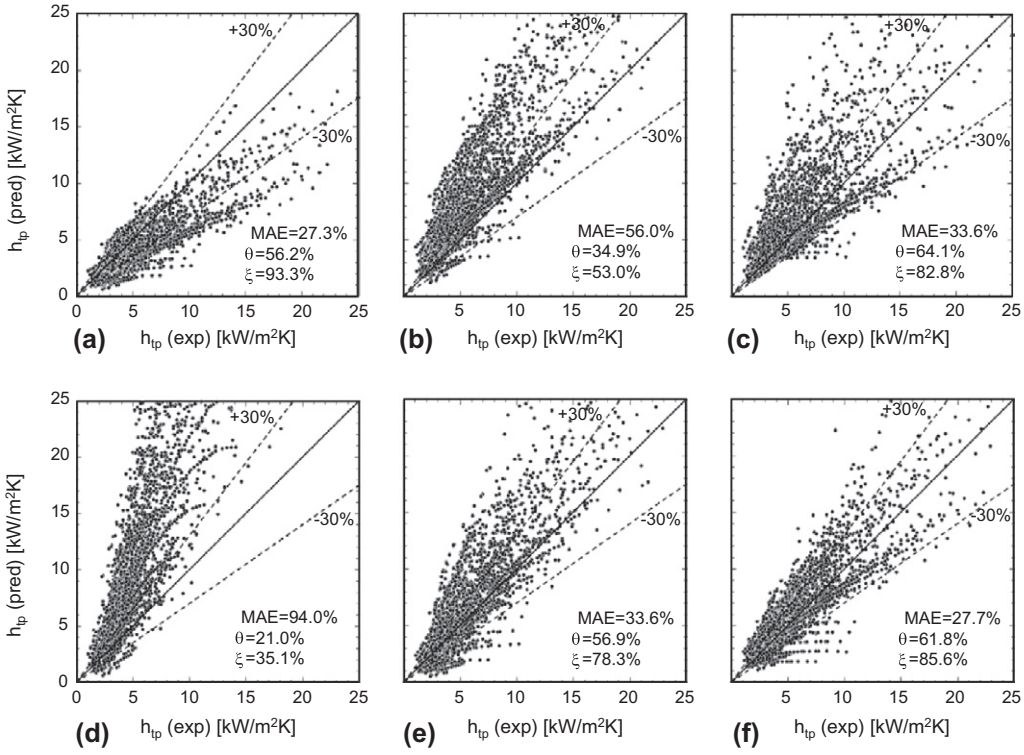

Fig. 2. Comparison of 3332 data points of the 4045 point consolidated database corresponding to annular condensation (smooth-laminar, wavy-laminar, transition to slug) in mini/micro-channels ($We^* > 7X_{tt}^{0.2}$) with predictions of annular flow condensation correlations recommended for macro-channels: (a) Akers and Rosson [44], (b) Cavallini and Zecchin [45], (c) Shah [46], (d) Haraguchi et al. [47], (e) Dobson and Chato [48], and (f) Moser et al. [49].

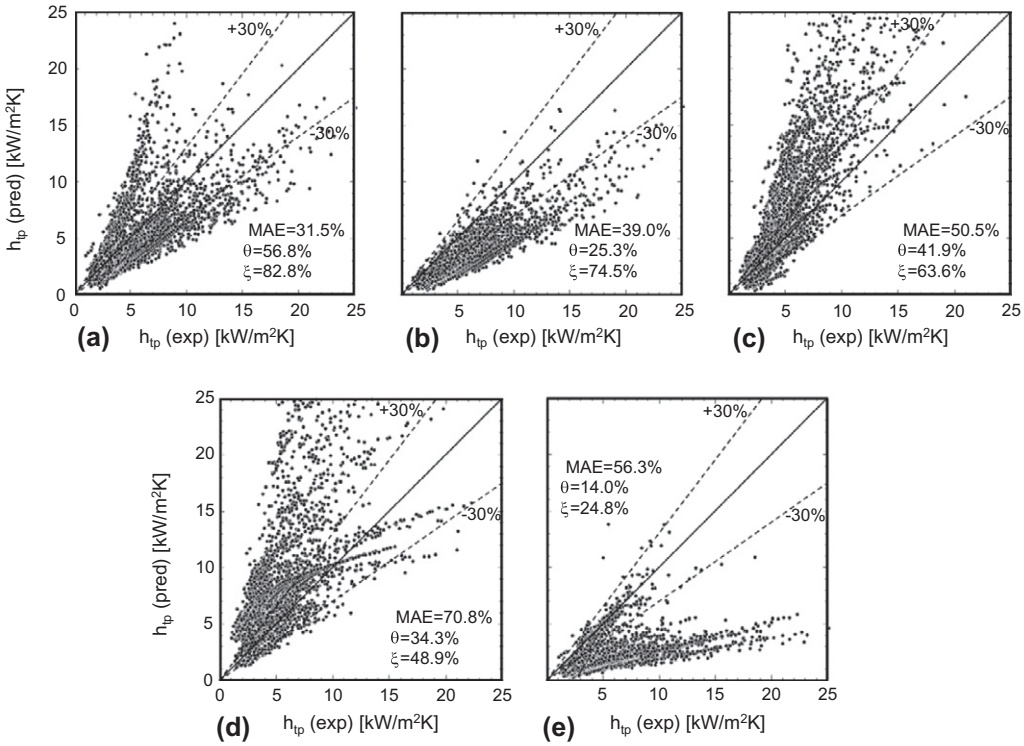

Fig. 3. Comparison of 3332 data points of the 4045 point consolidated database corresponding to annular condensation (smooth-laminar, wavy-laminar, transition to slug) in mini/micro-channels ($We^* > 7X_{tt}^{0.2}$) with predictions of annular flow condensation correlations recommended for mini/micro-channels: (a) Wang et al. [50], (b) Koyama et al. [51], (c) Huang et al. [39], (d) Bohdal et al. [53], and (e) Park et al. [41].

data that those for mini/micro-channels. This suggests that, unlike non-annular flow regimes, there are no major differences in condensation behavior between small and large channels in the annular regime, which consists of a liquid film that sheathes the channel walls, driven by the shear force exerted by the vapor core.

Table 2
Previous annular flow condensation heat transfer correlations.

Author (s)	Equation	Remarks
Akers and Rosson (1960)	$\frac{h_{tp}D_h}{k_f}=0.026\mathrm{Pr}_f^{1/3}\left\{G\left[(1-x)+x\left(\frac{\rho_f}{\rho_g}\right)^{0.5}\right]\frac{D_h}{\mu_f}\right\}^{0.8}$	D = 19.05 mm R12, propane $\mathrm{Re}_g\left(\frac{\mu_g}{\mu_f}\right)\left(\frac{\rho_f}{\rho_g}\right)^{0.5}>20{,}000, \mathrm{Re}_f>5{,}000$
Cavallini and Zecchin (1974)	$\frac{h_{tp}D_h}{k_f}=0.05\mathrm{Re}_f^{0.8}\mathrm{Pr}_f^{0.33}\left[1+\left(\frac{\rho_f}{\rho_g}\right)^{0.5}\left(\frac{x}{1-x}\right)\right]^{0.8}$	R12, R22, R113 $7000\leqslant \mathrm{Re}_{fo}\leqslant 53{,}000$
Shah (1979)	$\frac{h_{tp}D_h}{k_f}=0.023\mathrm{Re}_{fo}^{0.8}\mathrm{Pr}_f^{0.4}\left[(1-x)^{0.8}+\frac{3.8x^{0.76}(1-x)^{0.04}}{P_R^{0.38}}\right]$	D = 7–40 mm water, R11, R12, R22, R113, methanol, ethanol, benzene, toluene, trichloroethylene
Haraguchi et al. (1994)	$\frac{h_{tp}D_h}{k_f}=0.0152(1+0.6\mathrm{Pr}_f^{0.8})\frac{\phi_g}{X_{tt}}\mathrm{Re}_f^{0.77}X_{tt}=\left(\frac{\mu_f}{\mu_g}\right)^{0.1}\left(\frac{1-x}{x}\right)^{0.9}\left(\frac{v_f}{v_g}\right)^{0.5}\phi_g=1+0.5\left[\frac{G}{\sqrt{g\rho_g(\rho_f-\rho_g)D_h}}\right]^{0.75}X_{tt}^{0.35}$	D = 8.4 mm R22, R123, R134a
Dobson and Chato (1998)	$\frac{h_{tp}D_h}{k_f}=0.023\mathrm{Re}_f^{0.8}\mathrm{Pr}_f^{0.4}\left(1+\frac{2.22}{X_{tt}^{0.89}}\right)$	D = 3.14–7.04 mm R12, R22, R134a, R32/R125
Moser et al. (1998)	$\frac{h_{tp}D_h}{k_f}=\frac{0.0994^{C_1}\mathrm{Re}_f^{C_2}\mathrm{Re}_{eq}^{1+0.875C_1}\mathrm{Pr}_f^{0.815}}{(1.58lnRe_{eq}-3.28)(2.58lnRe_{eq}+13.7\mathrm{Pr}_f^{2/3}-19.1)}C_1=0.126\mathrm{Pr}_f^{-0.448}, C_2=-0.113\mathrm{Pr}_f^{-0.563}, \mathrm{Re}_{eq}=\phi_{fo,Friedel}^{8/7}\mathrm{Re}_{fo}$	D = 3.14–20 mm R11, R12, R125, R22, R134a, R410A
Wang et al. (2002)	$\frac{h_{tp}D_h}{k_f}=0.0274\mathrm{Pr}_f\mathrm{Re}_f^{0.6792}x^{0.2208}\frac{\phi_g}{X_{tt}}\phi_g^2=1.376+8X_{tt}^{1.665}$	D_h = 1.46 mm R134a multi-channel
Koyama et al. (2003)	$\frac{h_{tp}D_h}{k_f}=0.0152(1+0.6\mathrm{Pr}_f^{0.8})\frac{\phi_g}{X_{tt}}\mathrm{Re}_f^{0.77}\phi_g^2=1+21[1-exp(-0.319D_h)]X_{tt}+X_{tt}^2$	D_h = 0.80, 1.11 mm R134a multi-channel
Huang et al. (2010)	$\frac{h_{tp}D}{k_f}=0.0152(-0.33+0.83\mathrm{Pr}_f^{0.8})\frac{\phi_g}{X_{tt}}\mathrm{Re}_f^{0.77}\ \phi_g=\phi_{g,Haraguchi}$	D = 1.6, 4.18 mm R410A, R410A/oil
Bohdal et al. (2011)	$\frac{h_{tp}D}{k_f}=25.084\mathrm{Re}_f^{0.258}\mathrm{Pr}_f^{-0.495}P_R^{-0.288}\left(\frac{x}{1-x}\right)^{0.266}$	D = 0.31–3.30 mm R134a, R404A
Park et al. (2011)	$\frac{h_{tp}D}{k_f}=0.0055\mathrm{Pr}_f^{1.37}\frac{\phi_g}{X_{tt}}\mathrm{Re}_f^{0.7}\phi_g^2=1+13.17\left(\frac{\rho_g}{\rho_f}\right)^{0.17}\left[1-exp\left(-0.6\sqrt{\frac{g(\rho_f-\rho_g)D_h^2}{\sigma}}\right)\right]X_{tt}+X_{tt}^2$	D_h = 1.45 mm R134a, R236fa, R1234ze(E) multi-channel

4. New predictive method

4.1. Annular flow regimes (smooth annular, wavy-annular and transition to slug)

For a shear-dominated annular condensing flow, the local condensation heat transfer coefficient of the liquid film can be obtained from the following relation [43],

$$h_{ann}=\frac{q''_w}{T_{sat}-T_w}=\frac{\rho_f c_{p,f}u^*}{T_\delta^+}, \tag{4}$$

where the friction velocity and dimensionless boundary layer temperature are defined, respectively, as

$$u^*=\sqrt{\tau_w/\rho_f}, \tag{5}$$

and

$$T_\delta^+=\int_0^{\delta^+}\frac{q''}{q''_w}\left(\frac{1}{\mathrm{Pr}_f}+\frac{1}{\mathrm{Pr}_T}\frac{\varepsilon_m}{\nu_f}\right)^{-1}dy^+. \tag{6}$$

Table 3
Dimensionless groups employed in the prediction of condensation heat transfer.

Parameter	Definition	Interpretation
Nusselt number	$Nu_k=\frac{hD_h}{k_k}$, $k=f$ or g	$\frac{\text{Conduction resistance}}{\text{Convection resistance}}$
Liquid- or vapor-only Reynolds number	$\mathrm{Re}_{fo}=\frac{GD_h}{\mu_f}$ $\mathrm{Re}_{go}=\frac{GD_h}{\mu_g}$	$\frac{\text{Inertia}}{\text{Viscous force}}$ based on total flow rate
Superficial liquid or vapor Reynolds number	$\mathrm{Re}_f=\frac{G(1-x)D_h}{\mu_f}$ $\mathrm{Re}_g=\frac{GxD_h}{\mu_g}$	$\frac{\text{Inertia}}{\text{Viscous force}}$ based on actual flow rate for each phase
Prandtl number	$\mathrm{Pr}_k=\frac{\mu_k c_{p,k}}{k_k}$, $k=f$ or g	$\frac{\text{Momentum diffusivity}}{\text{Thermal diffusivity}}$
Density ratio	$\frac{\rho_f}{\rho_g}$	$\frac{\text{Liquid density}}{\text{Vapor density}}$
Weber number	$We=\frac{G^2D_h}{\rho_f\sigma}$	$\frac{\text{Inertia}}{\text{Surfacetension force}}$
Liquid- or vapor-only Suratman number	$Su_{fo}=\frac{\rho_f\sigma D_h}{\mu_f^2}\left(=\frac{\mathrm{Re}_{fo}^2}{We}\right)$ $Su_{go}=\frac{\rho_g\sigma D_h}{\mu_g^2}\left(=\frac{\mathrm{Re}_{go}^2}{We}\right)$	–
Froude number	$Fr=\frac{G^2}{gD_h\rho_f^2}$	$\frac{\text{Inertia}}{\text{Body force}}$
Bond number	$Bo=\frac{g(\rho_f-\rho_g)D_h^2}{\sigma}$	$\frac{\text{Bouyancy force}}{\text{Surfacetension force}}$
Galileo number	$Ga=\frac{\rho_f g(\rho_f-\rho_g)D_h^3}{\mu_f^2}$	–
Kapitza number	$Ka=\frac{\mu_f^4 g}{\rho_f\sigma^3}$	–
Jakob number	$Ja=\frac{c_{p,f}(T_{sat}-T_w)}{h_{fg}}$	$\frac{\text{Sensible heat}}{\text{Latent heat}}$
Lockhart–Martinelli parameter	$X_{vv}=\left(\frac{\mu_f}{\mu_g}\right)^{0.5}\left(\frac{1-x}{x}\right)^{0.5}\left(\frac{\rho_g}{\rho_f}\right)^{0.5}$ $X_{vt}=\left(\frac{f_f}{f_g}\right)^{0.5}\left(\frac{1-x}{x}\right)^{1.0}\left(\frac{\rho_g}{\rho_f}\right)^{0.5}$ $X_{tv}=\left(\frac{f_f}{f_g}\right)^{0.5}\left(\frac{1-x}{x}\right)^{1.0}\left(\frac{\rho_g}{\rho_f}\right)^{0.5}$ $X_{tt}=\left(\frac{\mu_f}{\mu_g}\right)^{0.1}\left(\frac{1-x}{x}\right)^{0.9}\left(\frac{\rho_g}{\rho_f}\right)^{0.5}$	Based on laminar liquid–laminar turbulent (vv), laminar liquid–turbulent vapor (vt), turbulent liquid–laminar vapor (tv), turbulent liquid–turbulent vapor (tt), where f_f and f_g are given by Eq. (13).

Table 4
New condensation heat transfer correlation method for mini/micro-channels in both single and multi-channel configurations. The pressure drop predictions are based on Ref. [75].

For annular flow (smooth-annular, wavy-annular, transition) where $We^* > 7X_{tt}^{0.2}$:
$\frac{h_{ann}D_h}{k_f} = 0.048\mathrm{Re}_f^{0.69}\mathrm{Pr}_f^{0.34}\frac{\phi_g}{X_{tt}}$.
For slug and bubbly flows where $We^* < 7X_{tt}^{0.2}$:
$\frac{h_{non-ann}D_h}{k_f} = [(0.048\mathrm{Re}_f^{0.69}\mathrm{Pr}_f^{0.34}\frac{\phi_g}{X_{tt}})^2 + (3.2\times10^{-7}\mathrm{Re}_f^{-0.38}Su_{go}^{1.39})^2]^{0.5}$.

where $X_{tt} = \left(\frac{\mu_f}{\mu_g}\right)^{0.1}\left(\frac{1-x}{x}\right)^{0.9}\left(\frac{\rho_g}{\rho_f}\right)^{0.5}$
$\phi_g^2 = 1 + CX + X^2$, $X^2 = \frac{(dP/dz)_f}{(dP/dz)_g}$,
$-\left(\frac{dP}{dz}\right)_f = \frac{2f_f v_f G^2(1-x)^2}{D_h}$,
$-\left(\frac{dP}{dz}\right)_g = \frac{2f_g v_g G^2 x^2}{D_h}$,
$f_k = 16\mathrm{Re}_k^{-1}$ for $\mathrm{Re}_k < 2000$,
$f_k = 0.079\mathrm{Re}_k^{-0.25}$ for $2000 \leqslant \mathrm{Re}_k < 20,000$,
$f_k = 0.046\mathrm{Re}_k^{-0.2}$ for $\mathrm{Re}_k \geqslant 20,000$,
For laminar flow in rectangular channel ($\beta < 1$),
$f_k\mathrm{Re}_k = 24(1 - 1.3553\beta + 1.9467\beta^2 - 1.7012\beta^3 + 0.9564\beta^4 - 0.2537\beta^5)$,
where subscript k denotes f or g for liquid and vapor phases, respectively,
$\mathrm{Re}_f = \frac{G(1-x)D_h}{\mu_f}$, $\mathrm{Re}_g = \frac{GxD_h}{\mu_g}$, $\mathrm{Re}_{fo} = \frac{GD_h}{\mu_f}$, $Su_{go} = \frac{\rho_g\sigma D_h}{\mu_g^2}$.

Liquid	Vapor (gas)	C
Turbulent	Turbulent	$0.39\mathrm{Re}_{fo}^{0.03}Su_{go}^{0.10}\left(\frac{\rho_f}{\rho_g}\right)^{0.35}$ for $\mathrm{Re}_f \geqslant 2000, \mathrm{Re}_g \geqslant 2000$ (tt)
Turbulent	Laminar	$8.7\times10^{-4}\mathrm{Re}_{fo}^{0.17}Su_{go}^{0.50}\left(\frac{\rho_f}{\rho_g}\right)^{0.14}$ for $\mathrm{Re}_f \geqslant 2000, \mathrm{Re}_g < 2000$ (tv)
Laminar	Turbulent	$0.0015\mathrm{Re}_{fo}^{0.59}Su_{go}^{0.19}\left(\frac{\rho_f}{\rho_g}\right)^{0.36}$ for $\mathrm{Re}_f < 2000, \mathrm{Re}_g \geqslant 2000$ (vt)
Laminar	Laminar	$3.5\times10^{-5}\mathrm{Re}_{fo}^{0.44}Su_{go}^{0.50}\left(\frac{\rho_f}{\rho_g}\right)^{0.48}$ for $\mathrm{Re}_f < 2000, \mathrm{Re}_g < 2000$ (vv)

The wall shear stress can be expressed as a function of the single-phase frictional pressure gradient based on gas flow using Lockhart and Martinelli's [72] two-phase multiplier approach,

$$\tau_w = -\left(\frac{dP}{dz}\right)_g \frac{D_h}{4}\phi_g^2 = 0.023\mathrm{Re}_g^{-0.2}G^2x^2v_g\phi_g^2. \tag{7}$$

Assuming the dimensionless temperature T_δ^+ is a function of Re_f and Pr_f, which is based on the functional forms proposed by Dobson and Chato [48] and Traviss et al. [73], yields the following general form for local heat transfer coefficient for annular condensing flow,

$$\frac{h_{ann}D_h}{k_f} = C_1 Re_f^{N_1} Pr_f^{N_2}\frac{\phi_g}{X_{tt}}, \tag{8}$$

where the two-phase pressure drop multiplier based on gas flow and the conventional turbulent–turbulent Lockhart–Martinelli parameter are given by

$$\phi_g^2 = 1 + CX + X^2, \tag{9}$$

and

$$X_{tt} = \left(\frac{\mu_f}{\mu_g}\right)^{0.1}\left(\frac{1-x}{x}\right)^{0.9}\left(\frac{\rho_g}{\rho_f}\right)^{0.5}, \tag{10}$$

respectively. Note that Eq. (9) uses the general definition of the Lockhart–Martinelli parameter, $X = \sqrt{(dP/dz)_f/(dP/dz)_g}$, and not X_{tt}. The general expression for X is based on the frictional pressure gradients based on actual flow rates for the individual phases,

$$-\left(\frac{dP}{dz}\right)_f = \frac{2f_f v_f G^2(1-x)^2}{D_h} \tag{11a}$$

and

$$-\left(\frac{dP}{dz}\right)_g = \frac{2f_g v_g G^2 x^2}{D_h}, \tag{11b}$$

and the Reynolds number and friction factor are determined separately for each phase, also based on the actual flow rate of the individual phase.

$$\mathrm{Re}_f = \frac{G(1-x)D_h}{\mu_f} \quad \text{for liquid,} \tag{12a}$$

$$\mathrm{Re}_g = \frac{GxD_h}{\mu_g} \text{ for vapor,} \tag{12b}$$

$$f_k\mathrm{Re}_k = 16 \text{ for } \mathrm{Re}_k < 2,000, \tag{13a}$$

$$f_k = 0.079\mathrm{Re}_k^{-0.25} \text{ for } 2,000 \leqslant \mathrm{Re}_k < 20,000, \tag{13b}$$

and

$$f_k = 0.046\mathrm{Re}_k^{-0.2} \text{ for } \mathrm{Re}_k \geqslant 20,000, \tag{13c}$$

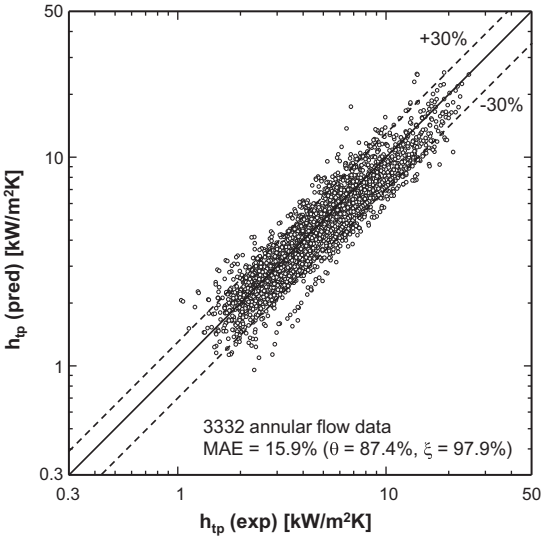

Fig. 4. Comparison of predictions of new annular flow condensation heat transfer correlation, Eq. (16), with 3332 data points of the 4045 point consolidated database corresponding to annular condensation (smooth-laminar, wavy-laminar, transition to slug) in mini/micro-channels ($We^* > 7X_{tt}^{0.2}$).

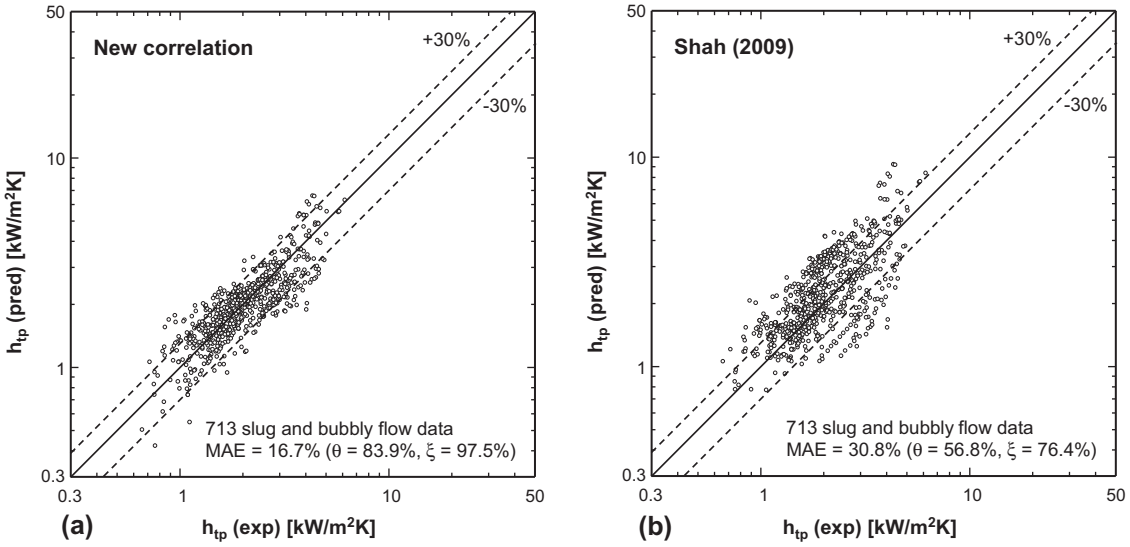

Fig. 5. Comparison of 713 data points of the 4045 point consolidated database corresponding to slug and bubbly flow condensation in mini/micro-channels ($We^* < 7X_{tt}^{0.2}$) with: (a) new correlation for slug and bubbly flow, Eq. (18), and (b) Shah [52].

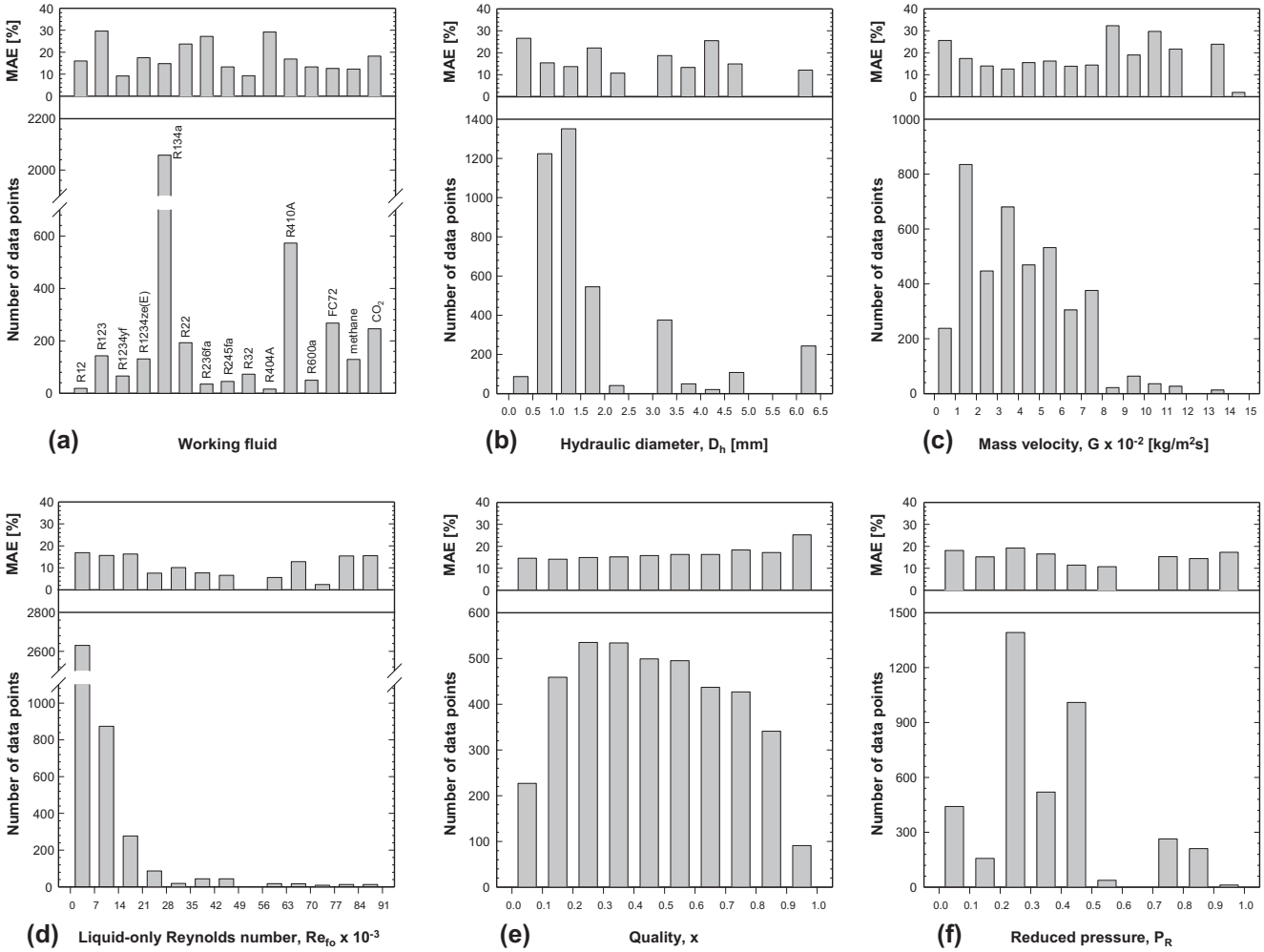

Fig. 6. Distributions of number of data points and MAE in predictions of new correlation method for entire 4045 point database relative to: (a) working fluid, (b) hydraulic diameter, (c) mass velocity, (d) liquid-only Reynolds number, (e) quality, and (f) reduced pressure.

where the subscript k denotes f for liquid or g for vapor. For laminar flow in rectangular channels, the two-phase friction factor can be obtained from [71],

$$f_k \mathrm{Re}_k = 24(1 - 1.3553\beta + 1.9467\beta^2 - 1.7012\beta^3 + 0.9564\beta^4 - 0.2537\beta^5). \quad (14)$$

Table 3 summarizes dimensionless groups that have been used in the past in the prediction of the condensation heat transfer coefficient. Most of these groups are essentially different combinations of inertia, viscous force, surface tension force and body (or buoyancy) force. What distinguishes mini/micro-channels from macro-channels is the strong influence of surface tension and viscosity, and negligible body force effects for the former as pointed out by Qu and Mudawar [74] and Kim and Mudawar [62]. This implies that the Froude, Bond, and Galileo numbers in Table 3 must be excluded from consideration when correlating mini/micro-channel condensation data.

Using the original formulation of Lockhart and Martinelli [72], Kim and Mudawar [75] proposed a new universal approach to predicting two-phase frictional pressure drop for adiabatic and condensing mini/micro-channel flows, replacing the constant C in the Lockhart–Martinelli parameter with a function of dimensionless groups from Table 4 that capture the influence of small channel size. The pressure drop predictions in [75] were validated against a consolidated database consisting of 7115 frictional pressure drop data points from 36 sources. The pressure drop correlations from [75] are provided in Table 4.

Kim and Mudawar [43] proposed that condensing flow in mini/micro-channels is annular (smooth-annular, wavy-annular, and transition to slug) for $We^* > 7X_{tt}^{0.2}$ and slug for $We^* < 7X_{tt}^{0.2}$, where the modified Weber number is defined by Soliman [76] as

$$We^* = 2.45 \frac{\mathrm{Re}_g^{0.64}}{Su_{go}^{0.3}(1 + 1.09X_{tt}^{0.039})^{0.4}} \text{ for } \mathrm{Re}_f \leqslant 1250, \quad (15a)$$

and

$$We^* = 0.85 \frac{\mathrm{Re}_g^{0.79} X_{tt}^{0.157}}{Su_{go}^{0.3}(1 + 1.09X_{tt}^{0.039})^{0.4}} \left[\left(\frac{\mu_g}{\mu_f} \right)^2 \left(\frac{\upsilon_g}{\upsilon_f} \right) \right]^{0.084} \text{ for } \mathrm{Re}_f > 1250. \quad (15b)$$

Table 5
Comparison of individual mini/micro-channel condensation heat transfer databases with predictions of present and select previous correlations.

Author(s)	Fluid(s)	Mean absolute error (%)							
		Annular flow data*					Slug and bubbly flow data		
		Datapoints	Akers and Rosson (1960)	Moser et al. (1998)	Wang et al. (2002)	New correl. Eq. (16)	Data points	Shah (2009)	New correl. Eq. (18)
Dobson et al. (1993a)	R134a, R12	73	28.7	17.6	29.8	13.3	3	19.2	2.9
Dobson et al. (1993b)	R22	29	36.8	17.1	44.0	20.8	3	13.9	8.7
Dobson (1994)	R134a, R22	150	40.4	12.8	44.3	27.3	15	15.3	16.2
Hirofumi and Webb (1995)	R134a	61	12.9	39.1	12.3	14.6	1	29.9	5.1
Zhang (1998)	R134a, R22, R404A	79	31.0	10.5	33.0	21.3	1	3.8	1.8
Wang (1999)	R134a	524	13.4	30.0	9.4	7.4	224	42.0	12.7
Yan and Lin (1999)	R134a	60	40.3	12.1	21.0	11.3	18	18.5	13.9
Baird et al. (2003)	R123	140	24.3	24.1	47.8	30.0	3	7.1	7.4
Kim et al. (2003)	R410A, R22	19	13.1	28.5	16.8	8.9	–	–	–
Jang and Hrnjak (2004)	CO_2	78	16.1	32.9	32.1	10.8	7	7.7	13.0
Cavallini et al. (2005)	R410A, R134a	56	30.3	12.7	33.4	19.1	3	7.0	13.6
Mitra (2005)	R410A	144	24.1	56.2	34.6	12.0	–	–	–
Shin and Kim (2005)	R134a	160	37.5	19.6	20.6	17.7	77	31.4	26.0
Andresen (2006)	R410A	312	23.8	55.2	47.9	16.0	3	69.1	68.1
Bandhauer et al. (2006)	R134a	116	25.9	15.1	15.1	10.0	12	30.6	15.6
Agra and Teke (2008)	R600a	50	46.6	16.6	17.5	13.3	-	-	-
Kim et al. (2009)	CO_2	42	15.8	39.1	25.9	15.6	6	31.2	12.6
Marak (2009)	Methane	124	14.9	24.2	32.0	12.4	5	25.3	8.3
Matkovic et al. (2009)	R134a, R32	131	32.7	14.0	34.5	15.6	30	26.6	11.4
Park and Hrnjak (2009)	CO2	78	13.1	43.5	13.9	26.7	35	39.1	20.9
Agarwal et al. (2010)	R134a	38	23.9	25.2	13.5	13.5	5	51.6	24.4
Bortolin (2010)	R245fa, R134a	241	43.1	13.6	30.0	22.4	68	20.9	17.7
Del Col et al. (2010)	R1234yf	56	27.5	8.6	16.3	9.1	10	12.8	10.0
Huang et al. (2010)	R410A	35	37.7	15.7	48.0	31.6	–	–	–
Oh and Son (2011)	R22, R134a, R410A	108	31.4	24.1	33.6	25.1	–	–	–
Park et al. (2011)	R134a, R236fa, R1234ze	117	20.0	30.8	18.4	19.1	87	21.3	15.0
Derby et al. (2012)	R134a	72	24.2	28.0	10.1	12.9	68	30.8	22.1
Kim and Mudawar (2012)	FC-72	239	44.7	30.4	86.6	11.8	29	19.4	19.6
Total		3332	27.3	27.7	31.5	15.9	713	30.8	16.7

* Annular flow data (smooth-annular, wavy-annular and transition to slug) corresponding to $We^* > 7X_{tt}^{0.2}$.

Based on 3332 data points from the consolidated 4045 point condensation heat transfer mini/micro-channel database corresponding to $We^* > 7X_{tt}^{0.2}$, the following new correlation for local annular condensing flow is obtained by fitting values for the coefficient and two exponents of Eq. (8),

$$\frac{h_{ann}D_h}{k_f} = 0.048\mathrm{Re}_f^{0.69}\mathrm{Pr}_f^{0.34}\frac{\phi_g}{X_{tt}}. \quad (16)$$

Fig. 4 shows this new annular correlation predicts the 3332 annular data points with a MAE of 15.9%, with 87.4% and 97.9% of the data falling within ±30% and ±50% error bands, respectively. Detailed relations needed to determine ϕ_g in Eq. (16) according to [75] are provided in Table 4.

4.2. Slug and bubbly flow regimes

For the slug and bubbly flows, the following functional form for local condensation heat transfer coefficient is proposed,

$$\frac{h_{non-ann}D_h}{k_f} = \left[\left(\frac{h_{ann}D_h}{k_f}\right)^{N_3} + \left(C_2\mathrm{Re}_f^{N_4}Su_{go}^{N_5}\right)^{N_3}\right]^{1/N_3}, \quad (17)$$

which is a superposition of the Churchill and Usagi [77] type of the new annular flow heat transfer correlation presented earlier, Eq. (16), and a dimensionless function of the superficial liquid Reynolds number, Re_f, and vapor-only Suratman number, Su_{go}.

Based on the present 713 of the 4045 data points of the consolidated database corresponding to $We^* < 7X_{tt}^{0.2}$, regression analysis yielded the following condensation heat transfer correlation for the slug and bubbly flow regimes,

$$\frac{h_{non-ann}D_h}{k_f} = \left[\left(0.048\mathrm{Re}_f^{0.69}\mathrm{Pr}_f^{0.34}\frac{\phi_g}{X_{tt}}\right)^2 + \left(3.2\times10^{-7}\mathrm{Re}_f^{-0.38}Su_{go}^{1.39}\right)^2\right]^{0.5}. \quad (18)$$

Fig. 5(a) and (b) compare the 713 slug and bubbly flow data points from 23 sources with predictions of the present correlation, Eq. (18), and Shah's [52] popular condensation heat transfer correlation, respectively. The Shah correlation is a modified version of his original annular flow correlation [46], covering a broader range of parameters and including slug and bubbly flows and high reduced pressures. Fig. 5(a) shows the present correlation predicts the slug and bubbly flow data with a MAE of 16.7%, with 83.9% and 97.5% of the data falling within ±30% and ±50% error bands, respectively. The corresponding values for the Shah correlation are a MAE of 30.8%, with 56.8% and 76.4% of the data falling within ±30% and ±50% error bands, respectively, indicating far greater deviation from the data compared to the new correlation.

Achieving low MAE values is an incomplete measure of the effectiveness of a correlation. A more definitive measure is predictive accuracy over broad ranges of individual flow parameters. As discussed in [65,66], this notion is overlooked in most studies involving the development of two-phase pressure drop and heat transfer correlations.

Fig. 6 shows, for each parameter, both a lower bar chart distribution of number of data points, and corresponding upper bar chart distribution of MAE in the prediction of the new condensation heat transfer correlations, which are summarized in Table 4. The distribution of the entire 4045 point database is examined relative to working fluid, hydraulic diameter, D_h, mass velocity, G, liquid-only Reynolds number, Re_{fo}, quality, x, and reduced pressure, P_R. Overall, the new correlation shows very good predictions for most parameter bins, with MAE values generally smaller than 20%. This shows that the accuracy of the new correlations is not compromised over the ranges of individual parameters.

Another measure of the predictive accuracy of the new correlation is the ability to provide evenly good predictions for individual databases comprising the consolidated database. Table 5 compares individual mini/micro-channel databases from 28 sources with predictions of the present correlations as well as select previous correlations that have shown relatively superior predictive capability as discussed earlier. For the annular flow data, the correlation of Moser et al. [49] provides good predictions compared to the previous correlations, but shows poor predictions of high reduced pressure data. The new annular flow correlation, Eq. (16), provides good predictions for all individual databases, with 14 databases predicted more accurately than by any of the previous correlations, and the best overall MAE of 15.9%. For the slug and bubbly flow regimes, the new correlation, Eq. (18), provides good predictions for all individual databases, with MAE values less than 20%, and the best overall MAE of 16.7%. One exception to this predictive accuracy is the 3 slug and bubbly flow data points of Andresen [29]. However, it should be noted that some of Andresen's low flow rate data show strong departure from the majority of comparable data.

Fig. 7(a) and (b) show predictions of the new correlations compared to two subsets of the consolidated database: multi-channel

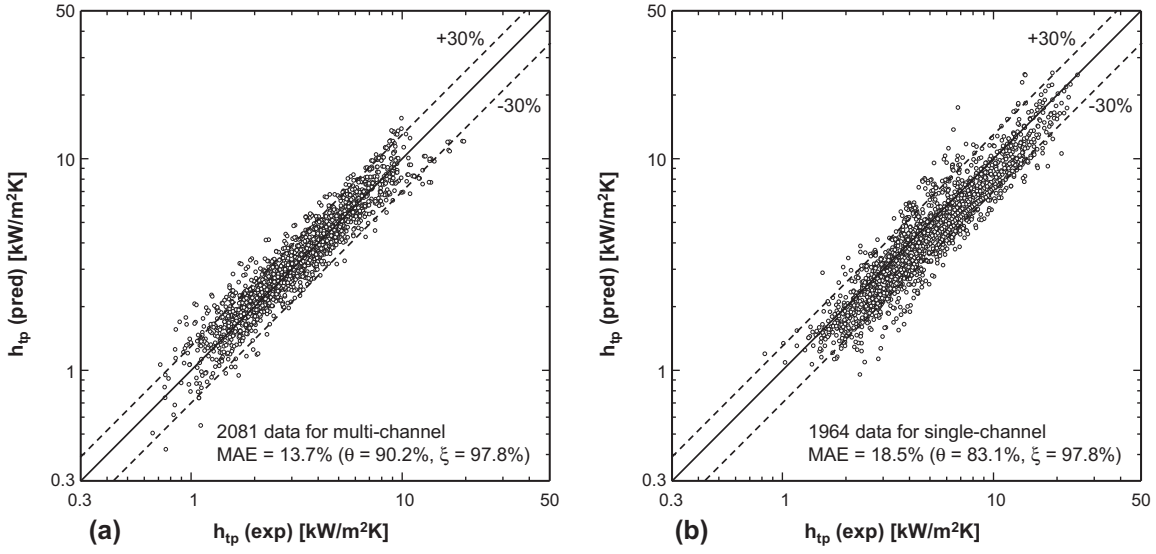

Fig. 7. Comparison of predictions of new correlations summarized in Table 4 with two subsets of the consolidated database corresponding to: (a) multi-channels and (b) single-channels.

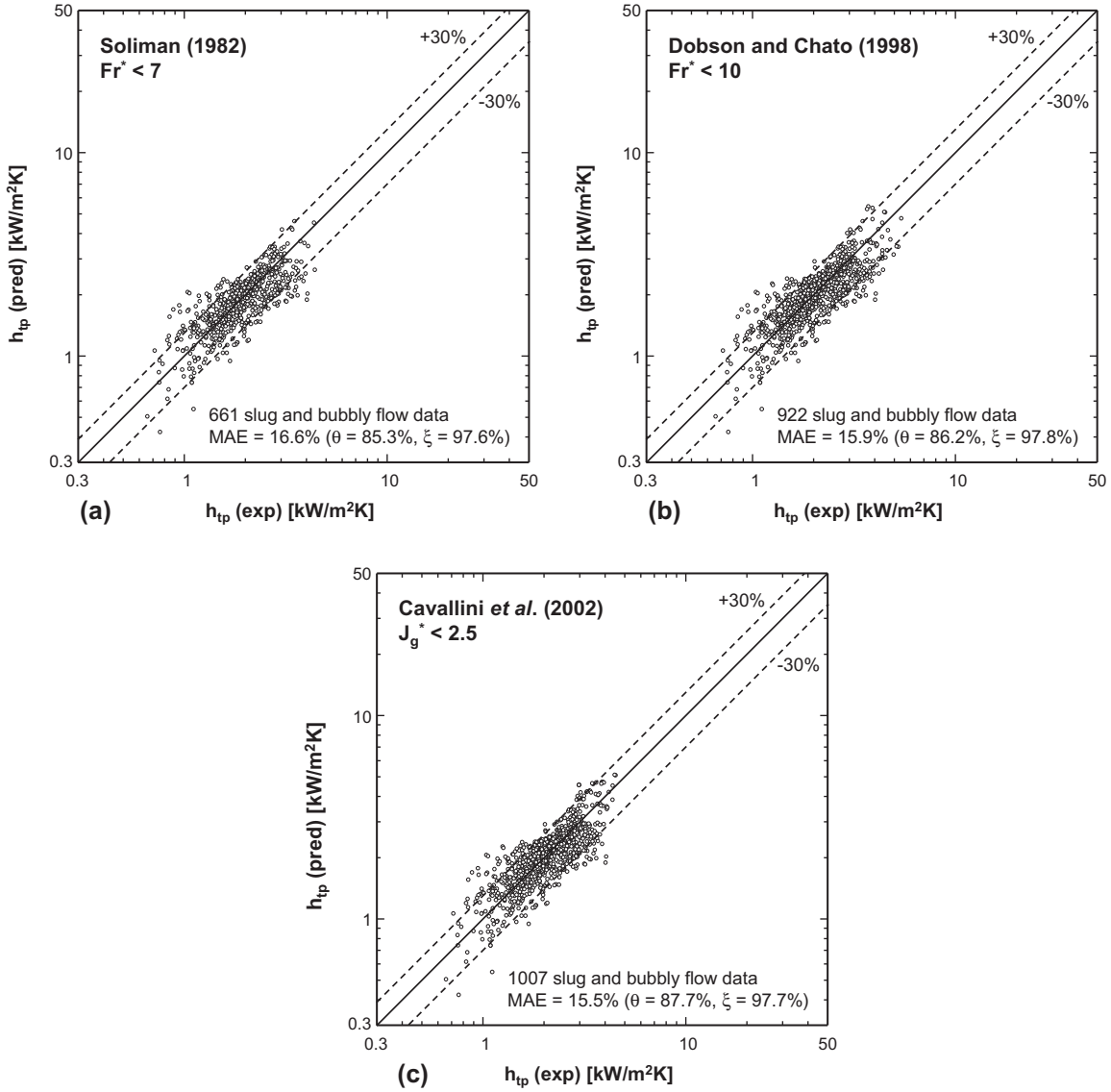

Fig. 8. Comparison of predictions of new slug and bubbly flow condensation heat transfer correlation, Eq. (18), with experimental data corresponding to: (a) $Fr^* < 7$ by Soliman [78], (b) $Fr^* < 10$ by Dobson and Chato [48], and (c) $J_g^* < 2.5$ by Cavallini et al. [79].

flow and flow in single channels, respectively. The MAE for the 2081 multi-channel data subset is 13.7%, with 90.2% and 97.8% of the data falling within ±30% and ±50% error bands, respectively. The corresponding values for the 1964 single-channel data subset are a MAE of 18.5%, and 83.1% and 97.8% of the data falling within ±30% and ±50% error bands, respectively. The overall MAE based on the entire 4045 point database is 16.0%, with 86.8% and 97.8% of the data falling within ±30% and ±50% error bands, respectively.

To further explore the accuracy of the new slug and bubbly flow correlation, the effects of different flow regime boundaries are examined. Fig. 8 compares the predictive accuracy of the new correlation against slug and bubbly flow data corresponding to different flow regime boundaries by Soliman [78], Dobson and Chato [48], and Cavallini et al. [79], respectively. Soliman proposed that the annular flow occurs when $Fr^* > 7$, and slug and wavy flows when $Fr^* < 7$ based on condensation data for R12, R113, and water along 4.8–15.9 mm horizontal tubes, where the modified Froude number is defined by Soliman as

$$Fr^* = 0.025\frac{\mathrm{Re}_f^{1.59}}{\mathrm{Ga}^{0.5}}\left(\frac{1+1.09X_{tt}^{0.039}}{X_{tt}}\right)^{1.5} \quad \text{for } \mathrm{Re}_f \leqslant 1250, \tag{19a}$$

and

$$Fr^* = 1.26\frac{\mathrm{Re}_f^{1.04}}{\mathrm{Ga}^{0.5}}\left(\frac{1+1.09X_{tt}^{0.039}}{X_{tt}}\right)^{1.5} \quad \text{for } \mathrm{Re}_f > 1250. \tag{19b}$$

Based on experimental data corresponding to $Fr^* < 10$ for condensation of binary refrigerant mixtures along 3.14–7.04 mm horizontal tubes, Dobson and Chato [48] developed a heat transfer correlation for slug and wavy flows. Based on previous flow regime maps, Cavallini et al. [79] proposed that condensing flows are annular for $J_g^* > 2.5$, and turn slug and wavy-stratified for $J_g^* < 2.5$, where the dimensionless superficial vapor velocity is defined as

$$J_g^* = Gx\Big/\sqrt{\rho_g(\rho_g-\rho_g)gD_h}. \tag{20}$$

Fig. 8 shows that there is no significant difference in predictive accuracy of the new slug and bubbly flow correlation when using the present boundary ($We^* < 7X_{tt}^{0.2}$) for transition from annular to slug flow versus the previous transition boundaries. The number of slug and bubbly flow data based on $We^* < 7X_{tt}^{0.2}$ is slightly larger than that based on Soliman [78] and smaller than those based on Dobson and Chato [48] and Cavallini et al. [79]. The new correlation

provides excellent predictions of slug and bubbly flow data regardless of the transition boundary used.

With the success of the present correlation method in predicting the condensation heat transfer coefficient for mini/micro-channels, future efforts must pursue theoretical models that accurately capture both the influences of small channel size and detailed interfacial behavior of condensing flows. This will require constructing different models for the different condensation flow regimes. For the annular regime, models must address the influence of interfacial instabilities. Past studies involving adiabatic, heated and evaporating liquid films have shown that interfacial waves can have a profound influence on mass, momentum and heat transfer in the film [80–85]. A second fundamental issue is the dampening of turbulent fluctuations near the vapor–liquid interface [62,86]. These modeling efforts will require more sophisticated diagnostic techniques that can accurately measure annular film thickness and characterize interfacial waves [85,87]. For slug flow, new models are needed to better predict the shape, size and propagation velocity of slug flow bubbles.

5. Conclusions

The primary goal of this study is to develop a universal technique to predicting the condensation heat transfer coefficient for mini/micro-channel flows. This goal is accomplished by first amassing a consolidated database consisting of 4045 condensation data points for mini/micro-channels from 28 sources. The database consists of 2081 multi-channel data points from 13 sources and 1964 single-channel data points from 17 sources, and includes 17 different working fluids. Parameter ranges include hydraulic diameters from 0.424 to 6.22 mm, mass velocities from 53 to 1403 kg/m^{2}s, liquid-only Reynolds numbers from 276 to 89,798, qualities from 0 to 1, and reduced pressures from 0.04 to 0.91. Key findings from the study are as follows:

(1) The consolidated database was compared to predictions of previous condensation heat transfer correlations for both macro-channel and mini/micro-channel flows. Only the macro-channel correlations by Akers and Rosson [44] and Moser et al. [49] show fair predictions of the consolidated database, with MAE values of 27.3%, and 27.7%, respectively. However, the Akers and Rosson correlation generally underpredicts the data, while that of Moser et al. overpredicts the high reduced pressure data. Interestingly, prior correlations for mini/micro-channel flows generally show poor predictions of the data.

(2) A universal approach to predicting the condensation heat transfer coefficient for mini/micro-channel flows is proposed. Two separate correlations are derived, one for predominantly annular flows (smooth annular, wavy-annular, and transition), and the second for slug and bubbly flows. This approach shows excellent predictive capability, with an overall MAE of 16.0% for the entire 4045 point database, and 86.8% and 97.8% of the data falling within ±30% and ±50% error bands, respectively. Moreover, the accuracy is fairly even for different working fluids, and over broad ranges of hydraulic diameter, mass velocity, quality and pressure, and for both single and multiple mini/micro-channels.

References

[1] I. Mudawar, Assessment of high-heat-flux thermal management schemes, IEEE Trans-CPMT: Compon. Packag. Technol. 24 (2001) 122–141.

[2] I. Mudawar, Two-phase micro-channel heat sinks: theory, applications and limitations, ASME J. Electron. Packag. 133 (2011). 041002-2.

[3] I. Mudawar, K.A. Estes, Optimizing and predicting CHF in spray cooling of a square surface, ASME J. Heat Transfer 118 (1996) 672–680.

[4] L. Lin, R. Ponnappan, Heat transfer characteristics of spray cooling in a closed loop, Int. J. Heat Mass Transfer 46 (2003) 3737–3746.

[5] J.R. Rybicki, I. Mudawar, Single-phase and two-phase cooling characteristics of upward-facing and downward-facing sprays, Int. J. Heat Mass Transfer 49 (2006) 5–16.

[6] Y. Katto, M. Kunihiro, Study of the mechanism of burn-out in boiling system of high burn-out heat flux, Bull. JSME 16 (1973) 1357–1366.

[7] I. Mudawar, D.C. Wadsworth, Critical heat flux from a simulated electronic chip to a confined rectangular impinging jet of dielectric liquid, Int. J. Heat Mass Transfer 34 (1991) 1465–1480.

[8] D.C. Wadsworth, I. Mudawar, Enhancement of single-phase heat transfer and critical heat flux from an ultra-high-flux simulated microelectronic heat source to a rectangular impinging jet of dielectric liquid, ASME J. Heat Transfer 114 (1992) 764–768.

[9] M.E. Johns, I. Mudawar, An ultra-high power two-phase jet-impingement avionic clamshell module, ASME J. Electron. Packag. 118 (1996) 264–270.

[10] T.C. Willingham, I. Mudawar, Forced-convection boiling and critical heat flux from a linear array of discrete heat sources, Int. J. Heat Mass Transfer 35 (1992) 2879–2890.

[11] M.B. Bowers, I. Mudawar, High flux boiling in low flow rate, low pressure drop mini-channel and micro-channel heat sinks, Int. J. Heat Mass Transfer 37 (1994) 321–332.

[12] T.N. Tran, M.W. Wambsganss, D.M. France, Small circular- and rectangular-channel boiling with two refrigerants, Int. J. Multiphase Flow 22 (1996) 485–498.

[13] H.J. Lee, S.Y. Lee, Heat transfer correlation for boiling flows in small rectangular horizontal channels with low aspect ratios, Int. J. Multiphase Flow 27 (2001) 2043–2062.

[14] V. Khanikar, I. Mudawar, T. Fisher, Effects of carbon nanotube coating on flow boiling in a micro-channel, Int. J. Heat Mass Transfer 52 (2009) 3805–3817.

[15] S.M. Kim, J. Kim, I. Mudawar, Flow condensation in parallel micro-channels – Part 1: experimental results and assessment of pressure drop correlations, Int. J. Heat Mass Transfer 55 (2012) 971–983.

[16] M.K. Dobson, J.C. Chato, D.K. Hinde, S.P. Wang, Experimental evaluation of internal condensation of refrigerants R-134a and R-12, University of Illinois at Urbana-Champaign (1993a) ACRC TR-38.

[17] M.K. Dobson, J.C. Chato, S.P. Wang, D.K. Hinde, J.A. Gaibel, Initial condensation comparison of R-22 with R-134a and R-32/R-125, University of Illinois at Urbana-Champaign (1993b) ACRC TR-41.

[18] M.K. Dobson, J.C. Chato, J.P. Wattelet, J.A. Gaibel, M. Ponchner, P.J. Kenney, R.L. Shimon, T.c. Villaneuva, N.L. Rhines, K.A. Sweeney, D.G. Allen, T.T. Hershberger, Heat transfer and flow regimes during condensation in horizontal tubes, University of Illinois at Urbana-Champaign (1994) ACRC TR-57.

[19] H. Hirofumi, R.L. Webb, Condensation in extruded aluminum tubes, Penn State Research Report, Showa Aluminum Corporation, 1995.

[20] M. Zhang, A new equivalent Reynolds number model for vapor shear-controlled condensation inside smooth and micro-fin tubes, Ph.D. thesis, Pennsylvania State University, PA, 1998.

[21] W.W. Wang, Condensation and single-phase heat transfer coefficient and flow regime visualization in microchannel tubes for HFC-134a, MS thesis, Ohio State University, OH, 1999.

[22] Y.Y. Yan, T.F. Lin, Condensation heat transfer and pressure drop of refrigerant R-134a in a small pipe, Int. J. Heat Mass Transfer 42 (1999) 697–708.

[23] J.R. Baird, D.F. Fletcher, B.S. Haynes, Local condensation heat transfer rates in fine passages, Int. J. Heat Mass Transfer 46 (2003) 4453–4466.

[24] N.H. Kim, J.P. Cho, J.O. Kim, B. Youn, Condensation heat transfer of R-22 and R-410A in flat aluminum multi-channel tubes with or without micro-fins, Int. J. Refrigeration 26 (2003) 830–839.

[25] A. Cavallini, D.D. Col, L. Doretti, M. Matkovic, L. Rossetto, C. Zilio, Condensation heat transfer and pressure gradient inside multiport minichannels, Heat Transfer Eng. 26 (2005) 45–55.

[26] J. Jang, P.S. Hrnjak, Condensation of CO_2 at low temperature, University of Illinois at Urbana-Champaign (2004) ACRC CR-56.

[27] B. Mitra, Supercritical gas cooling and condensation of refrigerant R410A at near-critical pressures, Ph.D. thesis, Georgia Institute of Technology, GA, 2005.

[28] J.S. Shin, M.H. Kim, An experimental study of flow condensation heat transfer inside circular and rectangular mini-channels, Heat Transfer Eng. 26 (2005) 36–44.

[29] U.C. Andresen, Supercritical gas cooling and near-critical-pressure condensation of refrigerant blends in microchannels, Ph.D. thesis, Georgia Institute of Technology, GA, 2006.

[30] T.M. Bandhauer, A. Agarwal, S. Garimella, Measurement and modeling of condensation heat transfer coefficients in circular microchannels, ASME J. Heat Transfer 128 (2006) 1050–1059.

[31] O. Agra, I. Teke, Experimental investigation of condensation of hydrocarbon refrigerants (R600a) in a horizontal smooth tube, Int. Commun. Heat Mass Transfer 35 (2008) 1165–1171.

[32] Y.J. Kim, J. Jang, P.S. Hrnjak, M.S. Kim, Condensation heat transfer of carbon dioxide inside horizontal smooth and microfin tubes at low temperatures, ASME J. Heat Transfer 131 (2009) 021501.

[33] K.A. Marak, Condensation heat transfer and pressure drop for methane and binary methane fluids in small channels, Ph.D. thesis, Norwegian University of Science and Technology, Trondheim, 2009.

[34] M. Matkovic, A. Cavallini, D.D. Col, L. Rossetto, Experimental study on condensation heat transfer inside a single circular minichannel, Int. J. Heat Mass Transfer 52 (2009) 2311–2323.

[35] C.Y. Park, P.S. Hrnjak, CO_2 flow condensation heat transfer and pressure drop in multi-port microchannels at low temperatures, Int. J. Refrigeration 32 (2009) 1129–1139.
[36] A. Agarwal, T.M. Bandhauer, S. Garimella, Measurement and modeling of condensation heat transfer in non-circular microchannels, Int. J. Refrigeration 33 (2010) 1169–1179.
[37] S. Bortolin, Two-phase heat transfer inside minichannels, Ph.D. thesis, University of Padua, Italy, 2010.
[38] D. Del Col, D. Torresin, A. Cavallini, Heat transfer and pressure drop during condensation of the low GWP refrigerant R1234yf, Int. J. Refrigeration 33 (2010) 1307–1318.
[39] X. Huang, G. Ding, H. Hu, Y. Zhu, H. Peng, Y. Gao, B. Deng, Influence of oil on flow condensation heat transfer of R410A inside 4.18 mm and 1.6 mm inner diameter horizontal smooth tubes, Int. J. Refrigeration 33 (2010) 158–169.
[40] H.K. Oh, C.H. Son, Condensation heat transfer characteristics of R-22, R-134a, R-410A in a single circular microtube, Exp. Therm. Fluid Sci. 35 (2011) 706–716.
[41] J.E. Park, F. Vakili-Farahani, L. Consolini, J.R. Thome, Experimental study on condensation heat transfer in vertical minichannels for new refrigerant R1234ze(E) versus R134a and R236fa, Exp. Therm. Fluid Sci. 35 (2011) 442–454.
[42] M. Derby, H.J. Lee, Y. Peles, M.K. Jensen, Condensation heat transfer in square, triangular, and semi-circular mini-channels, Int. J. Heat Mass Transfer 55 (2012) 187–197.
[43] S.M. Kim, I. Mudawar, Flow condensation in parallel micro-channels – Part 2: Heat transfer results and correlation technique, Int. J. Heat Mass Transfer 55 (2012) 984–994.
[44] W.W. Akers, H.F. Rosson, Condensation inside a horizontal tube, Chem. Eng. Prog. Symp. 56 (1960) 145–149.
[45] A. Cavallini, R. Zecchin, A dimensionless correlation for heat transfer in forced convection condensation, Proc. Fifth Int. Heat Transfer Conf., vol. 3, Tyoko, Japan, 1974, pp. 309–313.
[46] M.M. Shah, A general correlation for heat transfer during film condensation inside pipes, Int. J. Heat Mass Transfer 22 (1979) 547–556.
[47] H. Haraguchi, S. Koyama, T. Fujii, Condensation of refrigerants HCFC 22, HFC 134a and HCFC 123 in a horizontal smooth tube (2nd report), Trans. JSME (B) 60 (1994) 245–252.
[48] M.K. Dobson, J.C. Chato, Condensation in smooth horizontal tubes, ASME J. Heat Transfer 120 (1998) 193–213.
[49] K.W. Moser, R.L. Webb, B. Na, A new equivalent Reynolds number model for condensation in smooth tubes, ASME J. Heat Transfer 120 (1998) 410–417.
[50] W.W. Wang, T.D. Radcliff, R.N. Christensen, A condensation heat transfer correlation for millimeter-scale tubing with flow regime transition, Exp. Therm. Fluid Sci. 26 (2002) 473–485.
[51] S. Koyama, K. Kuwahara, K. Nakashita, K. Yamamoto, An experimental study on condensation of refrigerant R134a in a multi-port extruded tube, Int. J. Refrigeration 24 (2003) 425–432.
[52] M.M. Shah, An improved and extended general correlation for heat transfer during condensation in plain tubes, HVAC&R Res. 15 (2009) 889–913.
[53] T. Bohdal, H. Charun, M. Sikora, Comparative investigations of the condensation of R134a and R404A refrigerants in pipe minichannels, Int. J. Heat Mass Transfer 54 (2011) 1963–1974.
[54] I. Mudawar, A.H. Howard, C.O. Gersey, An analytical model for near-saturated pool boiling CHF on vertical surfaces, Int. J. Heat Mass Transfer 40 (1997) 2327–2339.
[55] A.H. Howard, I. Mudawar, Orientation effects on pool boiling CHF and modeling of CHF for near-vertical surfaces, Int. J. Heat Mass Transfer 42 (1999) 1665–1688.
[56] J.E. Galloway, I. Mudawar, CHF mechanism in flow boiling from a short heated wall-part 1. Examination of near-wall conditions with the aid of photomicrography and high-speed video imaging, Int. J. Heat Mass Transfer 36 (1993) 2511–2526.
[57] J.E. Galloway, I. Mudawar, CHF mechanism in flow boiling from a short heated wall-part 2. Theoretical CHF model, Int. J. Heat Mass Transfer 36 (1993) 2527–2540.
[58] C.O. Cersey, I. Mudawar, Effects of heater length and orientation on the trigger mechanism for near-saturated flow boiling critical heat flux – I. Photographic study and statistical characterization of the near-wall interfacial features, Int. J. Heat Mass Transfer 38 (1995) 629–641.
[59] C.O. Cersey, I. Mudawar, Effects of heater length and orientation on the trigger mechanism for near-saturated flow boiling critical heat flux – II. Critical heat flux model, Int. J. Heat Mass Transfer 38 (1995) 643–654.
[60] J.C. Sturgis, I. Mudawar, Critical heat flux in a long, rectangular channel subjected to onesided heating – I. Flow visualization, Int. J. Heat Mass Transfer 42 (1999) 1835–1847.
[61] J.C. Sturgis, I. Mudawar, Critical heat flux in a long, rectangular channel subjected to onesided heating – II. Analysis of critical heat flux data, Int. J. Heat Mass Transfer 42 (1999) 1849–1862.
[62] S.M. Kim, I. Mudawar, Theoretical model for annular flow condensation in rectangular micro-channels, Int. J. Heat Mass Transfer 55 (2012) 958–970.
[63] I. Mudawar, M.B. Bowers, Ultra-high critical heat flux (CHF) for subcooled water flow boiling – I. CHF data and parametric effects for small diameter tubes, Int. J. Heat Mass Transfer 42 (1999) 1405–1428.
[64] D.D. Hall, I. Mudawar, Ultra-high critical heat flux (CHF) for subcooled water flow boiling – II. High-CHF database and design parameters, Int. J. Heat Mass Transfer 42 (1999) 1429–1456.
[65] D.D. Hall, I. Mudawar, Critical heat flux (CHF) for water flow in tubes – I. Compilation and assessment of world CHF data, Int. J. Heat Mass Transfer 43 (2000) 2573–2604.
[66] D.D. Hall, I. Mudawar, Critical heat flux (CHF) for water flow in tubes – II. Subcooled CHF correlations, Int. J. Heat Mass Transfer 43 (2000) 2605–2640.
[67] A. Agarwal, Heat transfer and pressure drop during condensation of refrigerants in microchannels, Ph.D. thesis, Georgia Institute of Technology, GA, 2006.
[68] E.W. Lemmon, M.L. Huber, M.O. McLinden, Reference fluid thermodynamic and transport properties – REFPROP Version 8.0, NIST, MD, 2007.
[69] W. Qu, I. Mudawar, Flow boiling heat transfer in two-phase micro-channel heat sinks–I. Experimental investigation and assessment of correlation methods, Int. J. Heat Mass Transfer 46 (2003) 2755–2771.
[70] J. Lee, I. Mudawar, Two-phase flow in high-heat-flux micro-channel heat sink for refrigeration cooling applications: Part II – heat transfer characteristics, Int. J. Heat Mass Transfer 48 (2005) 941–955.
[71] R.K. Shah, A.L. London, Laminar Flow Forced Convection in Ducts: A Source Book for Compact Heat Exchanger Analytical Data, Supl 1, Academic press, New York, 1978.
[72] R.W. Lockhart, R.C. Martinelli, Proposed correlation of data for isothermal two-phase, two-component flow in pipes, Chem. Eng. Prog. 45 (1949) 39–48.
[73] D.P. Traviss, W.M. Rohsenow, A.B. Baron, Forced-convection condensation inside tubes: a heat transfer equation for condenser design, ASHRAE Trans. 79 (1973) 157–165.
[74] I. Qu, Mudawar, transport phenomena in two-phase micro-channel heat sinks, ASME J. Electron. Packag. 126 (2004) 213–224.
[75] S.M. Kim, I. Mudawar, Universal approach to predicting two-phase frictional pressure drop for adiabatic and condensing mini/micro-channel flows, submitted to Int. J. Heat Mass Transfer.
[76] H.M. Soliman, The mist-annular transition during condensation and its influence on the heat transfer mechanism, Int. J. Multiphase Flow 12 (1986) 277–288.
[77] S.W. Churchill, R. Usagi, A general expression for the correlation of rates of transfer and other phenomena, AIChE J. 18 (1972) 1121–1128.
[78] H.M. Soliman, On the annular-to-wavy flow pattern transition during condensation inside horizontal tubes, Can. J. Chem. Eng. 60 (1982) 475–481.
[79] A. Cavallini, G. Censi, D.D. Col, L. Doretti, G.A. Longo, L. Rossetto, Condensation of halogenated refrigerants inside smooth tubes, HVAC&R Res. 8 (2002) 429–451.
[80] J.A. Shmerler, I. Mudawar, Local heat transfer coefficient in wavy free-falling turbulent liquid films undergoing uniform sensible heating, Int. J. Heat Mass Transfer 31 (1988) 67–77.
[81] J.A. Shmerler, I. Mudawar, Local evaporative heat transfer coefficient in turbulent free-falling liquid films, Int. J. Heat Mass Transfer 31 (1988) 731–742.
[82] T.H. Lyu, I. Mudawar, Statistical investigation of the relationship between interfacial waviness and sensible heat transfer to a falling liquid film, Int. J. Heat Mass Transfer 34 (1991) 1451–1464.
[83] T.H. Lyu, I. Mudawar, Determination of wave-induced fluctuations of wall temperature and convective heat transfer coefficient in the heating of a turbulent falling liquid film, Int. J. Heat Mass Transfer 34 (1991) 2521–2534.
[84] I. Mudawar, R.A. Houpt, Mass and momentum transport in falling liquid films laminarized at relatively high Reynolds numbers, Int. J. Heat Mass Transfer 36 (1993) 3437–3448.
[85] I. Mudawar, R.A. Houpt, Measurement of mass and momentum transport in wavy-laminar falling liquid films, Int. J. Heat Mass Transfer 36 (1993) 4151–4162.
[86] I. Mudawar, M.A. El-Masri, Momentum and heat transfer across freely-falling turbulent liquid films, Int. J. Multiphase Flow 12 (1986) 771–790.
[87] J.E. Koskie, I. Mudawar, W.G. Tiederman, Parallel-wire probes for measurement of thick liquid films, Int. J. Multiphase Flow 15 (1989) 521–530.